Bioorganic & Medicinal Chemistry 18 (2010) 1497–1506

Contents lists available at ScienceDirect

Bioorganic & Medicinal Chemistry

journal homepage: www.elsevier.com/locate/bmc

Interaction between double helix DNA fragments and the new antitumor agent sabarubicin, Men10755

Stefania Mazzini [a,*], Leonardo Scaglioni [a], Fabio Animati [b], Rosanna Mondelli [a,*]

[a] Dipartimento di Scienze Molecolari Agroalimentari, Università di Milano, via Celoria 2, 20133 Milano, Italy
[b] Menarini Ricerche, via Tito Speri 10, Pomezia (Roma), Italy

ARTICLE INFO

Article history:
Received 31 July 2009
Revised 5 January 2010
Accepted 6 January 2010
Available online 11 January 2010

Keywords:
Drug–DNA interactions
NMR spectroscopy
Sabarubicin
Topoisomerase II inhibitors

ABSTRACT

Among the disaccharide derivatives of the antitumor anthracycline doxorubicin, sabarubicin (Men10755) is more active and less cytotoxic than doxorubicin. It showed a strong in vivo antitumor activity in all preclinical models examined, in conjunction with a better tolerability, and is now in phase II clinical trials.
The interaction of sabarubicin and Men10749 (a similar disaccharide with a different configuration at C-4′ of the proximal sugar) with the hexanucleotides d(CGTACG)$_2$ and d(CGATCG)$_2$ was studied by a combined use of 2D-^{1}H and ^{31}P NMR techniques. Both ^{1}H and ^{31}P chemical shifts of imino protons and phosphates allowed to established the intercalation sites between the CG base pairs, as it occurs for other anthracyclines of the series. The dissociation rate constants (k_{off}) of the slow step of the intercalation process were measured for Men10755 and Men10749, by NMR NOE-exchange experiments. The increase of k_{off}, with respect of doxorubicin, showed that the intercalation process is significantly faster for both drugs, leading to an average residence time for sabarubicin into d(CGTACG)$_2$ sixfold shorter than for doxorubicin. This could give account of both higher cytoplasmic/nuclear ratio and lower cellular uptake of sabarubicin in comparison with doxorubicin and accordingly of the lower cytotoxicity of these disaccharide analogues.
A relevant number of NOE interactions allowed the structure of the complexes in solution to be derived through restrained MD calculations. NMR-DOSY experiments were performed with several drug/oligonucleotide mixtures in order to determine the structure and the dimension of the aggregates.

1. Introduction

Anthracyclines are one of the most widely used class of antitumor agents and doxorubicin is the most active drug of this class.[1] The mechanism of the antitumor and cytotoxic activity of doxorubicins,[2] as well as of many other intercalating agents, is generally accepted to occur via the interference with the function of topoisomerase II, a nuclear enzyme that regulates the DNA topology. In spite of many years of study, the mechanism by which these molecules mediate their relatively selective antitumor effects is not yet clear. Although DNA intercalation is necessary for the activity, the mode and the site of drug binding was considered more critical than the strength of the DNA binding. The sugar and the cyclohexene rings were suggested to play an important role in the formation and stabilization of the ternary complex (DNA-drug-topoisomerase II).[3,4] As the sugar moiety, which in the complex is located in the minor groove, appears critical for the activity, a number of disaccharide analogues of daunorubicin and doxorubicin, have been synthesized.[5] The suggestion that the sugar moiety is important to modulate the activity was confirmed by the outstanding potent antitumor activity of 3′-morpholinyl derivatives of doxorubicin,[6] however associated with a too high cytotoxicity.[4,7] The morpholinyl analogues apparently possess a mechanism of action that differs from that of the parent anthracyclines, as they poison also topoisomerase I.[8] They form very stable complex with DNA, with a high residence time into the double helix, an order of magnitude longer than for doxorubicin, when measured with model oligonucleotides.[9,10]

Among the disaccharide derivatives of the antitumor anthracycline doxorubicin, sabarubicin (Men10755), is more active and less cytotoxic than the parent compound. It showed an important in vivo antitumor activity in all preclinical models examined, including tumors resistant to doxorubicin, in conjunction with a better tolerability with respect to doxorubicin, and is now in phase II clinical trials.[11–13] In this compound (Scheme 1) the amino sugar (daunosamine) is distal from the aglycone, while the proximal sugar (fucose) has the doxorubicin configuration at C-4′ (i.e., 4′*S*), resulting in an axial orientation of daunosamine ring. The conformational preference at the glycosidic bond and the shape of ring A, determined in dimethylsulfoxide solution,[14] are similar as for doxo and related anthracyclines.[15,16] The binding constant to calf thymus DNA, measured by UV and fluorescence spectroscopy resulted equal to that of doxorubicin (10^{-6} M^{-1}) measured in the same conditions.[17] These parameters are known to be strongly

* Corresponding author. Tel.: +39 02 50316824; fax: +39 02 50316801.
E-mail address: Stefania.mazzini@unimi.it (S. Mazzini).

0968-0896/$ - see front matter © 2010 Elsevier Ltd. All rights reserved.
doi:10.1016/j.bmc.2010.01.012

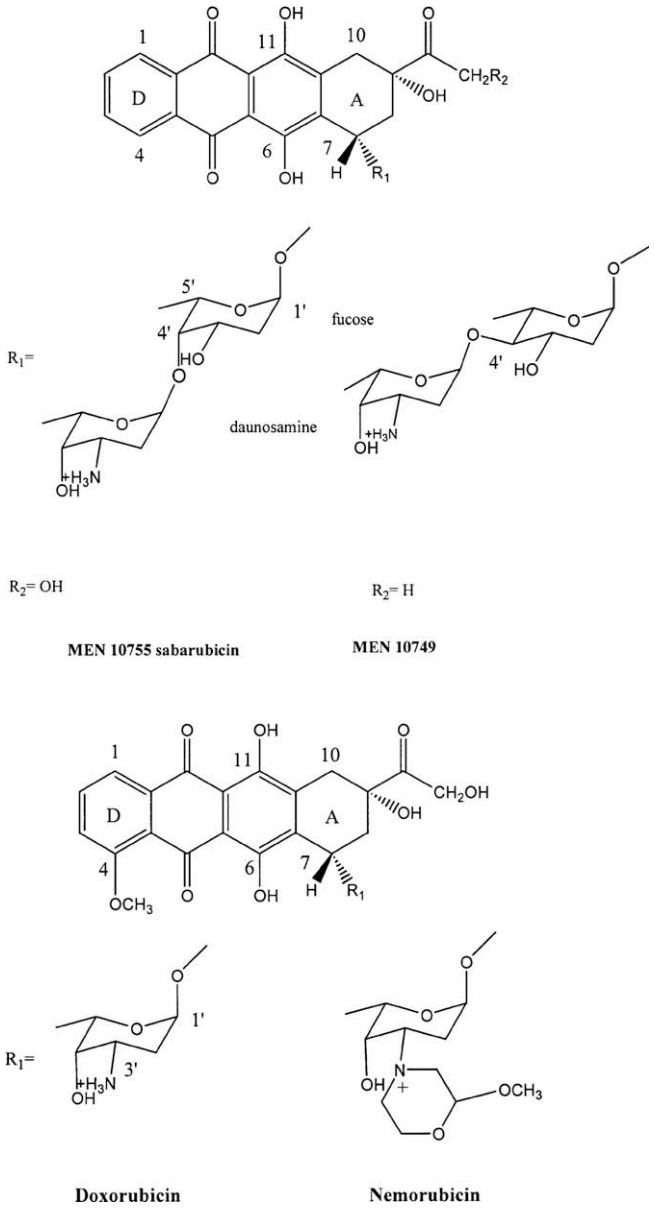

Scheme 1.

dependent on the non-specific ionic interactions with the negatively charged ionic surface of DNA, which always occurs with a positively charged ligand; in addition in this case, the strong self-association process might affect the measures. The X-ray analysis[18] of the complex formed between Men10755 and the model oligonucleotide d(CGATCG)$_2$ is more informative because it gives a detailed geometry of the complex: the structure is the same observed for other anthracyclines, that is, two drug molecules intercalated between the CG base pairs, with both sugar rings in the minor groove in one site, whereas in the other site the daunosamine moiety protrude out of the helix.

No study on the interaction in solution of disaccharides of this series with oligonucleotides has been reported so far. We thought that such an investigation by NMR experiments, in order to obtain information on the dynamic process of the intercalation could be of interest. The dissociation rate constants (k_{off}) of the slow step of the intercalation process can be measured with high accuracy directly by NMR NOE-exchange experiments[19] and were found not to depend upon ionic strength and self-association phenomena, as occurs for the binding constants. The kinetic constants ($1/k_{off}$) are an expression of the average residence time of the drug in the intercalation sites, a parameter which appeared to be related to the cytotoxic activity.[9,10]

We present here the study of sabarubicin, the most important compound of this series, in comparison with a disaccharide analogue of daunorubicin, Men10749. This latter, which has a 4′*S* configuration at C-4′ of fucose, was found[3] to be less active and less effective in stimulating topoisomerase II cleavage than sabarubicin. The NMR experiments were performed with the double helix oligonucleotides d(CGTACG)$_2$ and d(CGATCG)$_2$ henceforth referred as 'TA' and 'AT', respectively. Doxorubicin and daunorubicin are referred as doxo and dauno. With (I) is indicated the proximal sugar to the aglycone (fucose), with (II) the distal sugar (daunosamine).

2. Results and discussion

2.1. ^{1}H NMR experiments

^{1}H NMR titrations were performed in different conditions (see Section 4), but the best results were obtained in H_2O without salts. For both sabarubicin and Men10749 complexes all the protons of the bound species were attributed. Selected values are reported in Table 1, while the complete set of data are given in the Supplementary. The aromatic protons of the base pairs give two signals, due to the bound and free species, whereas the two resonances of the other protons are in general not well separated, leading often to broad signals.

Table 1
Selected ^{1}H chemical shift values for the complexes of sabarubicin with d(CGATCG)$_2$ and to d(CGTACG)$_2$[a]

d(CGATCG)$_2$ 15 °C bound to Men10755			$\Delta\delta$[b]
NHC_1G_6		13.04[c], 11.98[d]	−1.06
NHG_2C_5		12.80[c], 11.98[d]	−0.83
NHA_3T_4[e]		13.42[c], 12.96[d]	−0.56
2-H	A_3	7.79, 7.29	−0.50
8-H	A_3	8.37, 8.15	−0.22
8-H	G_2	7.99, 7.86	−0.13
8-H	G_6	7.94, 7.76	−0.18
6-H	C_1	7.74, 7.29	−0.45
6-H	C_5	7.40[e]	−0.22
6-H	T_4	7.17, 6.96	−0.21
5-H	C_1	5.80, 5,61	−0.19
5-H	C_5[f]	5.48, 5.19	−0.29
Drug			
6-OH		12.83[g], 12.18[d]	−0.64
11-OH		12.68[g], 11.74[d]	−0.94
d(CGTACG)$_2$ 10 °C bound to Men10755			$\Delta\delta$[h]
NHC_1G_6		13.04[c], 11.99[d] 11.80[d], 11.67[d]	−1.37
NHG_2C_5		12.84[c], 12.72[d] 12.15[d], 11.80[d]	−1.04
NHT_3A_4[e]		13.44[c], 13.26[d] 12.12[d], 13.09[d]	−0.35
Drug bound species			
6-OH		12.65, 12.54	−0.29
11-OH		12.16, 11.92	−0.76

[a] Measured from external DSS. Solvent H_2O–D_2O (90:10 v/v), pH 6.7, R = [ligand]/[DNA] = 2. Two signals, due to free and bound species were in general detected, unless otherwise specified.
[b] $\Delta\delta = \delta_{bound} - \delta_{free}$.
[c] Free species; the values are in general equal to those of the oligonucleotide in water.
[d] Bound species.
[e] Measured from the centre of a broad signal.
[f] Detected in D_2O for R = 1.
[g] The free species is absent. These values were obtained in the same conditions without the oligonucleotide.
[h] Maximum value.

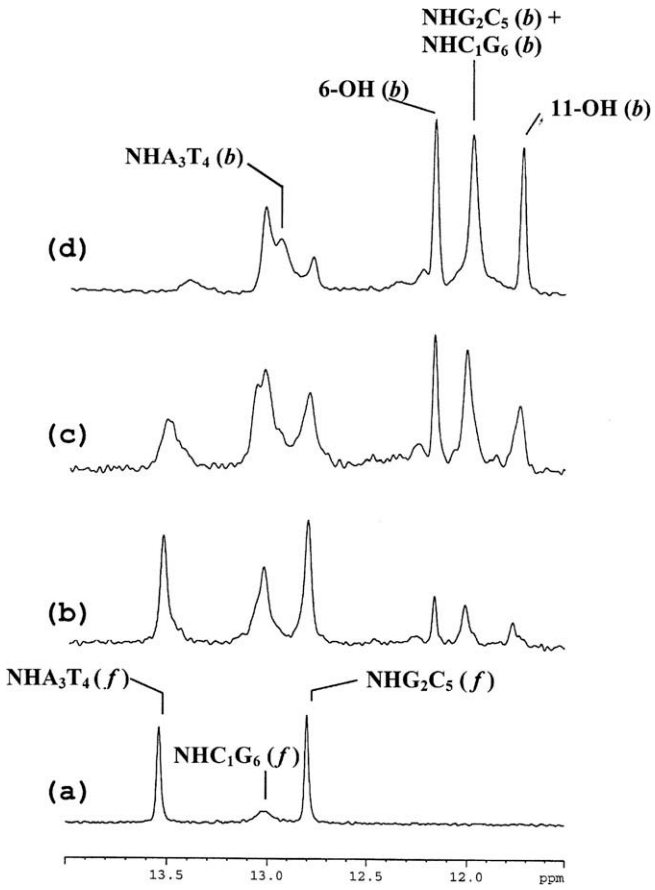

Figure 1. Low field region of ^{1}H NMR spectra in H_2O at 15 °C of sabarubicin/AT complex at different R = [drug]/[DNA]: (a) R = 0, (b) R = 0.5, (c) R = 1.0, (d) R = 2.0. The resonances belonging to the bound (b) and free (f) species are indicated.

The increase of the resonances of NH and OH protons belonging to the bound species can easily be followed during the titration experiments with sabarubicin, as shown in Figure 1. With *R = [drug]/[DNA]* = 2, the 6-OH and 11-OH signals of the drug are relatively sharp, as well as the imine protons NHG_2 C_5 and NHC_1G_6, whereas those of NHA_3T_4 are broader. The imine protons of the bound species are in slow exchange with those of the free species, still present in small amount, and were assigned by NOE interactions with the geminal NH_2 and the aromatic 6-H protons of cytidines C_5 and C_1 for NHG_2C_5 and NHC_1G_6, respectively, and by the NOE with 2-H(A_3) for NHA_3T_4. The 6-OH and 11-OH signals of the bound species lie at 12.18 and 11.74 ppm, respectively, those of the free drug were never detected, because of fast exchange with water, being no more protected by the double helix. They are indeed very broad even in the case of the free drug in very diluted water solution, were they appear at 12.83 and 12.68 ppm; in this case 6-OH was assigned at 12.83 ppm by the NOE cross-peak with H-7 in peri position on ring A of the drug. This interaction was not detected in the bound species, but inter-molecular NOEs of 11-OH with C_1 and G_2 protons were observed. Similar experiments were performed with Men10749.

The significant up field shift variation (0.8–1.0 ppm) found for the imine proton NHC_1G_6 and especially NHG_2C_5, suggests that the intercalating sites are between the CG base pairs, as observed in the solid state and as occurs for other doxorubicins. The complexes appear symmetrical, at least at the CG sites, while the very broad resonance of NHA_3T_4 suggests that in the minor groove the two molecules may assume different positions. A shielding of the same order was shown for the phenolic OH of the drugs, while the aromatic protons of both the drug and the base pairs show a generalized up field shift of 0.2–0.5 ppm.

We encountered more difficulties with TA complexes. All the resonances became very broad and did not simplify at $R \geqslant 2$. The spectra in H_2O at 10 °C showed two signals for each OH proton of the drug and four signals for each imine NH proton of the bases (Table 1). These latter were assigned to the mono-intercalated (two signals), to the bi-intercalated (one signal) and to the free species (one signal), which latter decreases during the titration. The two OH signals were both attributed to the bound species, as those of the free drug are not detectable.

These results are interpreted as follows: with AT the intercalation at both the CG sites is completed with R = 2, whereas in the case of the TA sequence the second drug molecule intercalates with much more difficulty, and consequently the mono-intercalated specie is more stable. The stoichiometry of two drugs per duplex can also be derived for the sabarubicin/AT complex from the UV spectra, which present two 'step' of intercalation for R = 1 and for R = 2–3, in agreement with the X-ray results, but in the case of TA the two steps are not visible.

2.2. ^{31}P NMR experiments

In order to confirm these results, we performed phosphorus experiments.

The chemical shift variation of the ^{31}P resonances should provide a unique evidence of an intercalation process. A geometrical deformation in the phosphodiester chain is generally induced by changes at the level of P-O(5′) and P–O(3′) bonds. For a B-DNA type oligomer, the values of the torsion angles α = O(3′)–P–O(5′)–C(5′) and ζ = C(3′)–O(3′)–P-O(5′) normally are −60° and −90°, respectively (*gauche–gauche* conformation), whereas the *gauche–trans* conformation (α = −60°, ζ = 180°), as a consequence of intercalation, is associated with a low-field shift up to 1.0–1.5 ppm.[9,10,20,21]

The titration experiments on AT with sabarubicin, performed at 15 °C, shows the appearance of a new signal at low field, which was assigned to C_5 pG_6 by 2D NOESY-exchange, as the assignment for the free nucleotide is known[22,23] ($\Delta\delta = \delta_{bound} - \delta_{free}$ = +1.09 ppm). The spectra reported in Figure 2 show the correlations between the signals belonging to the phosphates groups of the bound species (low field) in chemical exchange with those of the same groups in the free state. Other new signals appeared at low field, which were assigned to G_2pA_3 and/or C_1pG_2 (Table 2). The addition of sabarubicin to TA induces line broadening even with R = 0.2 at 25 °C as well as at lower temperatures. However, at 5 °C the resonance at low field of C_5pG_6 of the bound species could be detected. At room temperature the intercalation process is much faster and the signals are sharper; consequently we could not detect new signals, but it was possible to follow the progressive low field shift of all the phosphorus resonances during the titration experiment. In particular in the case of TA complex, we could follow C_1pG_2 and G_2pT_3, as they are well separated in the free oligonucleotide. The most deshielded are C_5pG_6 and G_2pT_3, with $\Delta\delta$ of +0.40 and +0.35 ppm, respectively, which shows that the deformation of the phosphodiester chains mainly affects these phosphate groups.

The titration with Men10749 was much more difficult: the very broad low field signal of C_5pG_6 was detected only in the case of AT complex, with a $\Delta\delta$ of +1.25 ppm. In the case of doxo and nemorubicin (methoxymorpholinodoxorubicin) we measured[10] for C_5pG_6 $\Delta\delta$ values of +1.5 and +1.2 ppm, respectively, with both oligonucleotides, but also G_2pA_3, with $\Delta\delta$ of +(0.8–1.0) ppm, appeared similarly affected. The strong conformational change of this latter phosphate must be due to the methoxy group on the chromophore, which is absent in sabarubicin.

These results are evidence of the intercalation between the CG base pairs for both drugs and show that the process is slightly more difficult for CGTA than for CGAT sequence.

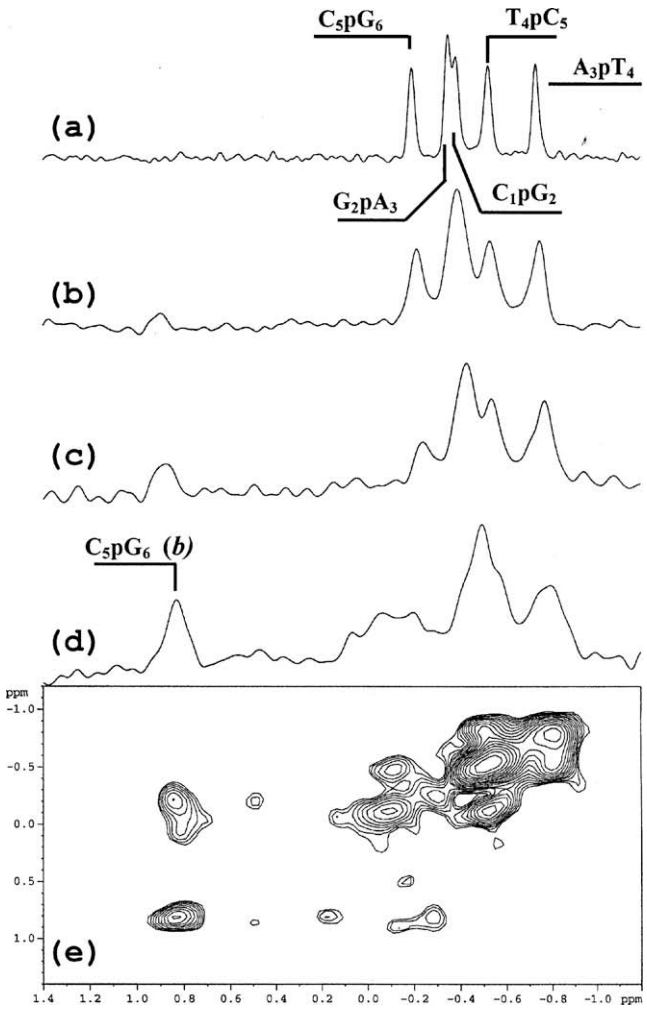

Figure 2. ^{1}H-decoupled ^{31}P NMR spectra at 15 °C of sabarubicin/AT complex with different R = [drug]/[DNA]: (a) R = 0, (b) R = 0.5, (c) R = 1.0, (d) R = 2.0; (e) 2D-^{31}P-NOESY exchange spectrum, R = 2.0, t_{mix} 150 ms. Cross peaks arise from chemical exchange of the phosphates between free and bound species.

Table 2
^{31}P chemical shift values for d(CGTACG)$_2$ and d(CGATCG)$_2$ bound to Men10755, Men10749 and doxorubicin[a]

Phosphate Group	Free **TA**[c]	Bound to δ_{bound}	Men10755 $\Delta\delta$	doxo[b] $\Delta\delta$
C_1pG_2	−0.43	−0.26	+0.17	+0.45
G_2pT_3	−0.74	−0.39	+0.35	+0.84
T_3pA_4	−0.51	−0.39	+0.12	−0.14
A_4pC_5	−0.54	−0.50	+0.04	−0.14
C_5pG_6	−0.49	+0.11	+0.40	+1.53
C_5pG_6[d]	−0.08	+0.90	+0.98	
[e]	AT	δ_{bound}	$\Delta\delta$	$\Delta\delta$
C_1pG_2	−0.33	−0.43[f]	−0.10	+0.43
G_2pA_3	−0.31	0.00[f]	+0.31	+1.53
A_3pT_4	−0.70	−0.38	+0.32	⩽0.2
T_4pC_5	−0.50	−0.51	−0.01	⩽0.2
C_5pG_6	−0.19	+0.90	+1.09	+1.57
	Free	Bound to	Men10749	
[e]	**AT**	δ_{bound}	$\Delta\delta$	
C_5pG_6	−0.11	+1.14	+1.25	

[a] Measured in ppm(δ) and referenced from external MDA set at 16.8 ppm. Solvent D_2O, pH 6.7, 10 mM phosphate buffer, 0.1 M NaCl, R = 2, except for Men10749 performed with R = 1.5. $\Delta\delta = \delta_{bound} - \delta_{free}$.
[b] Taken at 25 °C from Ref. 15.
[c] 25 °C.
[d] 5 °C.
[e] 15 °C.
[f] The assignments may be interchanged.

Table 3
Dissociation rate constants (k_{off}) and averaged life time ($1/k_{off}$) for the AT- and TA-complexes with anthracyclines[a]

Drug	TA-complex		AT-complex	
	k_{off} (s^{-1})	$1/k_{off}$ (s)	k_{off} (s^{-1})	$1/k_{off}$ (s)
Men10749	5.4 ± 3.6[b]	0.18 ± 0.11	5.6 ± 0.6[b]	0.18 ± 0.02
Men10755	4.6 ± 0.45[b]	0.21 ± 0.025	2.1 ± 0.1[b]	0.47 ± 0.03
Men10755	—	—	1.8 ± 0.4[c]	0.55 ± 0.12
Doxorubicin	0.8 ± 0.3[b]	1.25 ± 0.46	1.2 ± 0.04[b]	0.83 ± 0.03
Nemorubicin	0.2 ± 0.1[c]	5.00 ± 2.5	—	—

[a] Measured at 15 °C from ^{1}H spectra and ^{31}P spectra, in D_2O, pH 6.7, 10 mM phosphate buffer, 0.1 M NaCl.
[b] From ^{1}H spectra.
[c] From ^{31}P spectra.

2.3. Measure of the kinetic constants

The kinetic aspects of the interaction between sabarubicin and the two oligonucleotides were studied by means of 2D NOESY-exchange experiments on phosphorus and protons, following known procedure[19] previously used[9] to study this type of molecules. At 15 °C, most base proton resonances in the bound and free environments are both present for all R values, as they are in a relatively slow exchange regime. This was proved by TOCSY and ROESY experiments. As all the molecular species are in a dynamic equilibrium, it was possible to measure the dissociation rate constants (k_{off}) of the slow step of the intercalation process, which are 4.6 s^{-1} for sabarubicin–TA complex and 2.1 s^{-1} for AT-complex. The latter value was confirmed by ^{31}P experiments, which gave a k_{off} of 1.8 s^{-1}. Higher values, 5.4 and 5.6 s^{-1}, were measured for both complexes of Men10749 (see Table 3 and Fig. 2).

The same measurements were performed with doxo and nemorubicin in the same experimental conditions, in order to have the best comparison. The data in Table 3 shows that the kinetic of the intercalation process is significantly faster for sabarubicin than for doxo, leading to an average life time, $1/k_{off}$, into the TA intercalation sites of 0.21 s, which is six times shorter than for doxo, 1.25 s, and very much shorter with respect to the most cytotoxic molecule of this family, that is, nemorubicin, 5 s. The interaction with AT seems more preferred, as also appeared from the titration experiments, but the intercalation process remains faster for sabarubicin with respect to doxo. For Men10749 the process is even faster than for sabarubicin and is the same with both sequences.

2.4. DOSY experiments

The strong tendency of daunomycins to self-aggregate is well known.[9,24,25] The equilibrium constants for the dimerization process of anthracyclines of this series were found of the order of 10^4 M^{-1}, but larger aggregates might be present in solution, especially at the NMR concentrations. In the presence of DNA or oligonucleotides this process appears to be enhanced, otherwise the significant broadening of all the signals cannot be justified only with the intercalation process. It has been suggested[26,27] that the intercalation is preceded by a fast non-specific outside binding. As the structure and the dimensions of these aggregates were never investigated, several drug/TA and drug/AT mixtures were subjected to NMR DOSY experiments.[28]

The results (Table 4) show that all complexes with TA have a greater molecular weight (MW) than that corresponding to a bi-intercalated duplex, except for nemorubicin, where the value for the complex exactly corresponds to the MW of a duplex bound

Table 4
Diffusion coefficients (DC) and molecular weights (MW) for the AT- and TA-complexes with anthracyclines[a]

Complex with $d(CGTACG)_2$	DC ($m^2 s^{-1}$)	MW exp.	MW calcd	Composition duplex + drugs
Sabarubicin	−9.947	10.256	10.224	2 + 4
Men10749	−9.889	7.722	7.828	1 + 6
Doxorubicin	−9.863	6.704	6.649	1 + 5
Nemorubicin	−9.807	5.042	5.040	1 + 2
Complex with $d(CGATCG)_2$	DC (m^2s^{-1})	MW exp.	MW calcd	Composition duplex+drugs
Sabarubicin	−9.907	8.376	7.828	1 + 6
Men10749	−9.845	6.183	5.791	1 + 3
Doxorubicin	−9.080	4.874	4.912	1 + 2
Doxorubicin	−9.077	4.187	4.333	1 + 1

[a] Obtained by DOSY experiments at 25 °C in D_2O, 10 mM phosphate buffer, 0.1 M NaCl , pH 6.7, R = 2 except for Men10749/TA performed with R = 1.5. The calibration curve was obtained as described in Ref. 30.

to two drug molecules (5040). Actually, nemorubicin presents minimal aggregation phenomena and a strong anchorage to the double helix with a long residence time, which must be related to the position of the positive charge located on the morpholino ring. This bulky and hydrophobic moiety (with the cooperation of the methoxy substituent) strongly reduces the flexibility around the glycosidic bond, and at the same time, acts as a shielding for the positive charge, with the result of constraining the amino group inside into the minor groove, and thus non available for intermolecular interactions with an other duplex. For the same reasons, the external ionic interactions with the negative ionic surface of the oligonucleotide by this drug are significantly reduced.

On the contrary, for doxo, as well as for the disaccharide analogues, the positive charge of daunosamine ring is not constrained and can easily interact with the ionic surface of the duplex. The MW obtained for the doxo-TA complex corresponds to one duplex with five drug molecules, while for the complex with AT two values were obtained corresponding to a mono- and to a bi-intercalated duplex. Sabarubicin shows the most significant aggregation, which in the case of TA complex involves two duplex units, as can be represented in Figure 3. The axial orientation of the daunosamine ring in sabarubicin increases the flexibility of the sugar moieties, so much that in the solid phase[18] the charged daunosamine ring at the second site can protrude out of the minor groove. In solution, it is just the charged amino group of daunosamine that can link the two duplexes each other. Men10749, with equatorial orientation of the daunosamine ring, forms complexes with MW similar to those of doxorubicin. The absence of the hydroxyl group at C-14 has no importance, as the OH group is on the aglycone, the orientation of which is highly conserved through the two series.[29]

The aggregation phenomenon thus appears significantly more pronounced for TA- than for AT-complexes. The reason must be found in the increased stability of the latter ones, and specifically in the tighter binding of the amino sugar in AT- than in TA-complexes, as observed for dauno in the solid phase.[29] Consequently the amino group is less available for linking an other duplex unit, and in addition to the intercalation, free drug molecules may bind externally to the ionic surface of the duplex.

2.5. NOESY experiments and modeling

The ^{1}H NOESY spectra of the complexes with both oligonucleotides gave a relevant number of intermolecular interactions between the ligands and the duplexes and in general the lack of the sequential intra-molecular NOEs between G_2 and C_1 protons of the nucleotides. Some examples are reported in Figure 4 . At first we studied the AT-complexes, as the spectra are of a good quality and because a structure in the solid phase is known.[18]

The contacts of the anthraquinone moiety with C_5, C_1 and G_2 protons confirm for both drugs the intercalation sites between the CG base pairs of the helix. Specifically, the orientation of the aglycone is proved by the selective interactions between the aromatic protons and the cytidines, that is, H-1,4 with C_1 and H-2,3 with C_5. In addition, the contact of 8-CH_2 with H-1′(G_6) and for sabarubicin the interaction of 11-OH with guanine G_2 confirm this finding. The contacts in the minor groove are more interesting, because at this site the two intercalated drug molecules may assume different positions. The protons of both sugar moieties of sabarubicin show NOE interactions with A_3 and T_4. Specifically, the strong NOE of 5′-Me (II) with H-2 of adenine A_3 indicates that this portion of daunosamine is deeply inserted in the minor groove. This is confirmed by the additional interactions of 5′-Me (II) and H-5′(II) with H-1′ and H-5′5″ of T_4.

Driven by the experimental NOEs, two models were devised, with one molecule and with two molecules of sabarubicin intercalated between the terminal CG base pairs. The models were energy-minimized and subjected to a restrained molecular dynamics calculations (MD). No other restraints, except for the distances obtained from the NOE values and the hydrogen bonds between the DNA base pairs, were applied. In this way the double helix was allowed to move freely. Table 5 lists the NOE data and the distances values of the final structure obtained by MD for the bi-intercalated model (Fig. 5).

The position of the anthraquinone ring is similar for the mono- and the bi-intercalated models; ring D in the mono-intercalated structure is slightly closer to H-5 of C_1, while ring A is slightly more distant from the G_6 ribose ring. The orientation of the aglycone in both models is at 45° with respect to the base pairs, with the aro-

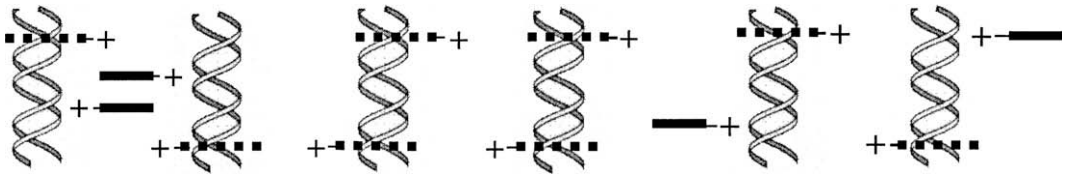

Figure 3. Schematic models of the molecular aggregate for sabarubicin/TA complex with R = [drug]/[DNA] = 2.0. The filled and dotted black bars represent sabarubicin molecules externally bound and intercalated in the double helix, respectively.

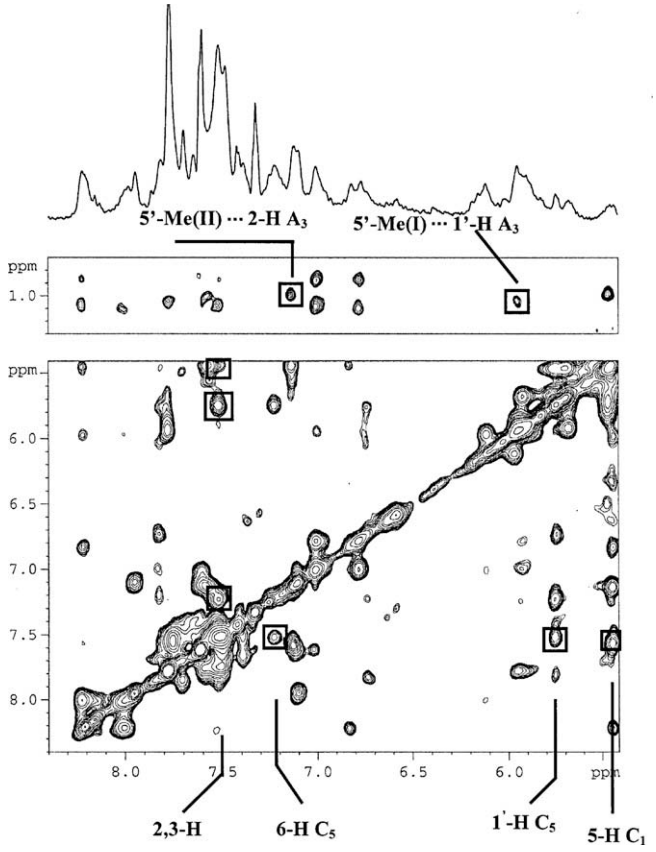

Figure 4. Selected region of 2D NOESY spectrum of sabarubicin/AT complex at 15 °C in H_2O, pH 6.7, R = 3.0, t_{mix} 300 ms. The NOE interactions are shown.

matic moiety parallel to the planes of the cytidines and guanines. Ring D is more deeply inserted into the duplex than in the X-ray structure,[18] as results from the NOE contacts between ring D and C_1 protons. The intercalation of the second drug molecule should induce significant conformational changes in the sugar moieties, as well as in the phosphoribose backbone. In order to discuss this point, it is better to take an overview of the α and ζ phosphodiester angles derived from MD by sampling the conformations every 1 ps. A selected display for AT-complex is reported in Figure 6, while the complete set of data are in the Supplementary. The most significant conformational changes around the phosphate bonds were observed for αG_2, αA_3, αG_6 and ζC_5 of strand A and for αG_2 and αG_6 of strand B, which values indicate predominantly *trans* conformations. In the minor groove all the conformations are *gauche–gauche*. These results are in good agreement with the strong down-field shift found for the phosphate resonances of C_5pG_6 and with the smaller deshielding for C_1pG_2 and G_2pA_3.

The flexibility of the sugar moiety in sabarubicin is mainly due to the rotation around the glycosidic bonds, because the conformation of both sugar rings is *chair*. The values of τ angles[†] obtained from the final structure derived by MD and reported in the Supplementary, correspond to a single structure, while in solution there is an equilibrium between different conformations. However, we can consider this structure as a good model of a preferred conformation, because it is in very good agreement with the experimental NOEs and ^{31}P data. The angles of the proximal sugar are equal at both sites, $\tau_1 \sim -70°$, $\tau_2 \sim 140°$, but differ from those of the predominant conformation of the free drug.[14] These angles correspond to ψ and φ values

[†] τ_1 = C(8)–C(7)–O(7)–C(1′); τ_2 = C(7)–O(7)–C(1′)–C(2′); τ_3 = C(3′)–C(4′)–O(4′)–C(1′); τ_4 = C(4′)–O(4′)–C(1′)–C(2′).

Table 5
Intermolecular NOE interactions and inter-proton distances (Å) for the complex of Men10755 with $d(CGATCG)_2$[a]

Men10755	$d(CGATCG)_2$		NOE[b]	d[c]	
				Site 1	Site 2
1,4-H[d]	5-H	C_1, C_7	m	3.7	3.5
1,4-H	6-H	C_1, C_7	m[e]	3.0	2.7
1,4-H	2′-H	C_1, C_7	m	2.6	4.8
1,4-H	2″-H	C_1, C_7	[f]	3.9	3.2
2,3-H[g]	5-H	C_1, C_7	m	3.7	3.6
2,3-H	5-H	C_5, C_{11}	s	2.7	3.6
2,3-H	6-H	C_5, C_{11}	s	3.6	3.7
2,3-H	1′-H	C_5, C_{11}	m[h]	5.3	5.2
2,3-H	2′-H	C_5, C_{11}	m	4.5[i]	4.4[i]
8-CH_2	1′-H	G_6, G_{12}	m	4.0,4.4	5.4,5.8
11-OH	1′-H	C_1, C_7	s	3.6	4.7
11-OH	1′-H	G_2, G_8	s	3.0	3.4
11-OH	2′-H	G_2, G_8	m[h]	5.5	9.1[l]
1′-H(I)	1′-H	G_6, G_{12}	m	5.0	4.7
1′-H(I)	2′-H	C_5, C_{11}	w	5.2	5.1
5′-Me(II)	5′5″-H	C_5,C_{11}	m	6.2[i]	4.3[i]
5′-Me(I)	2-H	A_3, A_9	m	4.7, 7.9	8.1, 5.0
5′-Me(I)	1′-H	A_3, A_9	w	3.6, 11.6	11.8, 6.2
5′-Me(II)	2- H	A_3, A_9	s	3.5, 4.1	3.5, 4.7
5′-Me(II)	1′-H	T_4, T_{10}	w	3.9, 5.8	7.7, 3.1
Relevant conformational energy parameters E (kcal/mol)					
Forcing				4.8	
Van der Waals				−183.2	
Hydrogen-bond				−10.0	
Coulomb				−102.1	
Total				72.6	
Distance violations (>0.3 Å)				4	6

[a] Acquired at 15 °C, solvent D_2O and H_2O–D_2O (90:10 v/v), pH 6.7 the solution in D_2O was added of 10 mM phosphate buffer and 0.1 M NaCl. 2′-H and 5′-H stand for low field, 2″-H and 5″H for up field proton.

[b] A quantification of the NOE intensities was estimated as follow: s = 2.5–3.5 Å, m = 3.5–4.5 Å, w = 4.5–5.5 Å.

[c] Obtained from the final structures of the complex after MD calculations. The distances are referred to the C_1–G_6 strand for site 1 and to the C_7–G_{12} strand for site 2, while for the minor groove sites both values are reported.

[d] 1-H and 4-H are coincident, the distances are referred to 1-H.

[e] Partially overlapped by other signals.

[f] Overlapped by the interaction between 8-H(G_6) and 2′-H(G_6).

[g] 2-H and 3-H are coincident, the distances to 5-H C_1 and C_7 are referred to 2-H, all the others to 3-H.

[h] With a component of secondary NOE.

[i,l] The distance is referred to *pro-R* ([i]) and *pro-S* ([l]), respectively.

of ~30° and ~170°, respectively, which are similar to those of a minor conformation, ψ = 37° and φ = 131°, found for the free drug.[14] By contrast, the glycosidic angles of daunosamine moiety are slightly different for the two sites, as can be seen in Figure 7. The intramolecular NOEs observed for the bound drug and reported in the Supplementary are in agreement with these conformations; in particular the interaction between 5′-Me (I) and H-5′(II) justifies the orientation of the daunosamine ring.

These results can be summarised as follows: the inter-molecular NOE interactions involving H-5′ and 5′-Me of daunosamine moiety with A_3 and T_4 protons determine the position of the drug in the minor groove. From these data it follows that the hydrophobic portion of both sugar rings, that is, the 5′-Me groups, is located deeply into the minor groove. Consequently the positively charged amino group of daunosamine becomes close (4.2 Å) to O-4′ of C_5 in one site, whereas in the other site it is more distant from all the ribose oxygen atoms of the backbone. Thus the charged NH_3^+ groups are on the boundary of the minor groove and can interact with the negative ionic surface of the helix and with the water molecule of the solvent. This differs from the X-ray structure, where the whole daunosamine ring of the second site protrudes out of the groove.

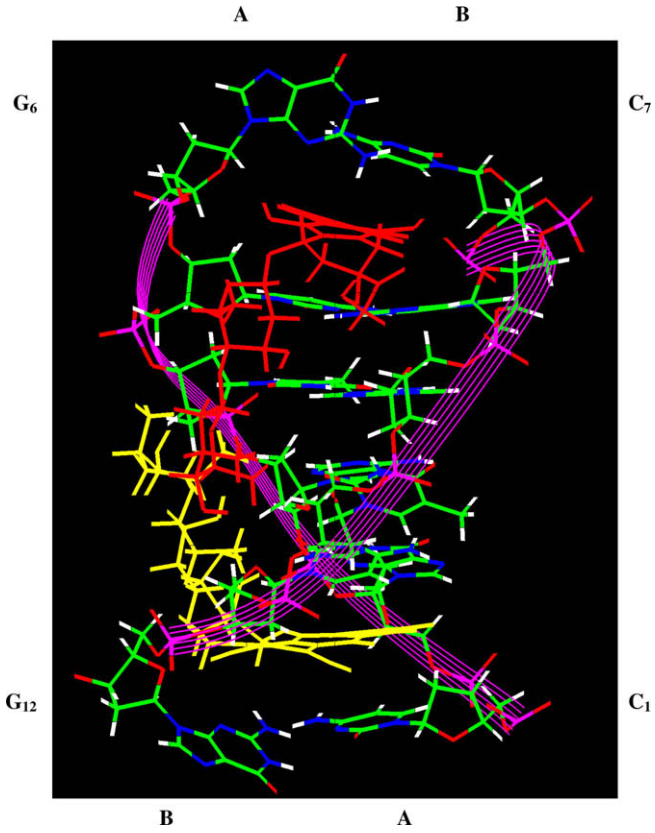

Figure 5. Energy minimized molecular model of the bi-intercalated complex between sabarubicin and AT. A represents strand from C_1 to G_6 and B strand from C_7 to G_{12}. The drug molecules at the site 1 and site 2 are yellow and red, respectively.

In the mono-intercalated model of sabarubicin/AT complex, the site of the phosphoribose backbone involved in the intercalation appears rather similar to that of the bi-intercalated model, with deformations of the angles αT_4 and ζC_5 of strand A and αG_2 and ζC_1 of strand B. The complex of sabarubicin with TA presents some interesting differences. The model, similarly derived from the NOE values reported in Table 6, shows *gauche–gauche* conformations for all phosphate, in agreement with the ^{31}P titration experiments. Also the very short residence time into the double helix is in line with the absence of deformations on the phosphodiester backbone. The conformation of the bound drug (Fig. 7) is different with respect to the AT-complex: the strong NOE between H-5′(I) and H-8 eq is an evidence of the rotation of fucose around the glycosidic bond, in agreement with the distance of 3.3 Å and with the values of the dihedral angles τ_1 (84°) and τ_2 (158°) derived from the final MD structure. The orientation of daunosamine ring follows from the contact (3.9 Å) of H-5′(I) with H-1′(II) and from the strong NOE interaction (2.7 Å) between H-1′(II) and Me(I). The inter-molecular NOEs between drug and TA protons in the minor groove involve 5′-Me(I) of fucose and T_3 protons, while daunosamine shows contacts with A_4 and C_5. Therefore, the two methyl groups are located on the two opposite walls of the groove and NH_3^+ is on the boundary of the minor groove, but more distant, compared with AT complex, from the oxygen atoms of the backbone (6.3 Å from O-4′(A_4), 9–16 Å from the others). This probably allows it to link an other duplex, as deduced from the DOSY experiments.

The complexes of Men10749 are similar for both oligomers. The NOE contacts of the aglycone moiety with C_1, C_5 and G_6 units, which characterise the intercalation into the CG base-pairs, were found for both complexes, together with the NOEs between 5′-Me of fucose and H-1′ of guanine G_6. In the minor groove of TA-complex there are many contacts involving fucose, T_3 protons and H-2(A_4) and the methyl group of daunosamine with H-3′(T_3). In the AT-complex, some interactions were found between fucose and A_3 protons. Nevertheless, the conformation at the phosphate angles are all *gauche–gauche* (with only ~50% of *trans* ζC_5), in agreement with the ^{31}P results. The conformation of the bound drug is also similar for both complexes, as shown by the values of τ angles at the glycosidic bonds. In Figure 7 we report the preferred conformation of Men10749 bound to AT, obtained from the NOE values reported in the Supplementary. Actually, the equatorial binding of daunosamine ring at C-4′(I) is responsible of the more closed shape of the disaccharide moiety. Consequently, the positively charged NH_3^+ group is close (3.7–4.8 Å) to the ribose oxygen atoms of the backbone, that is, C_5, T_{10} and C_{11} units for AT- and A_{10} and C_{11} for TA-complex, respectively.

3. Conclusions

The most interesting results of this study lie in the values of the averaged residence times into the intercalation sites, obtained for sabarubicin and other anthracyclines from the dissociation rate constants of the slow step of the intercalation process. The residence time of sabarubicin into $d(CGATCG)_2$ is one half, into $d(CGTACG)_2$ is six times shorter than for doxorubicin, and very much shorter with respect to the most cytotoxic molecule of these series, that is, nemorubicin. The interaction with AT seems more preferred, as also appeared from the titration experiments. For Men10749 the process is even faster than for sabarubicin and is the same with both sequences. This could give account of both

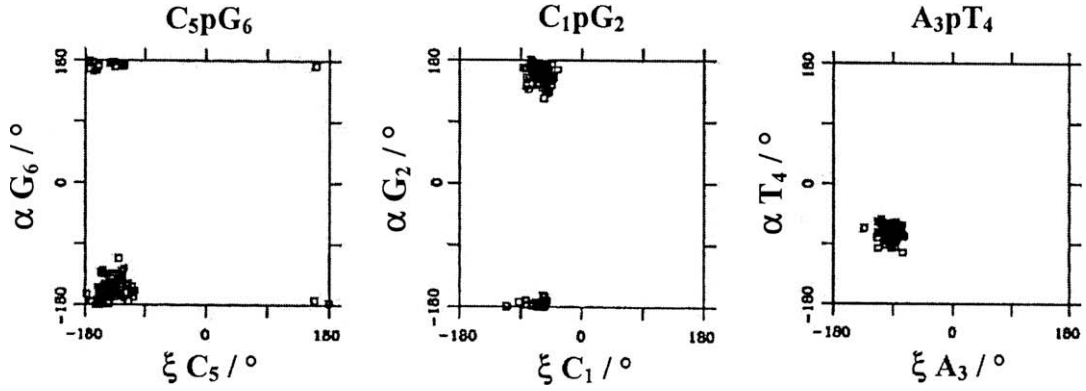

Figure 6. Selected examples of correlation between α and ζ torsion angles for the C_5pG_6 (strand A), C_1pG_2 and A_3pT_4 (strand B) phosphate groups in the sabarubicin/AT bi-intercalated complex, obtained from MD calculations. The complete set is reported in the Supplementary.

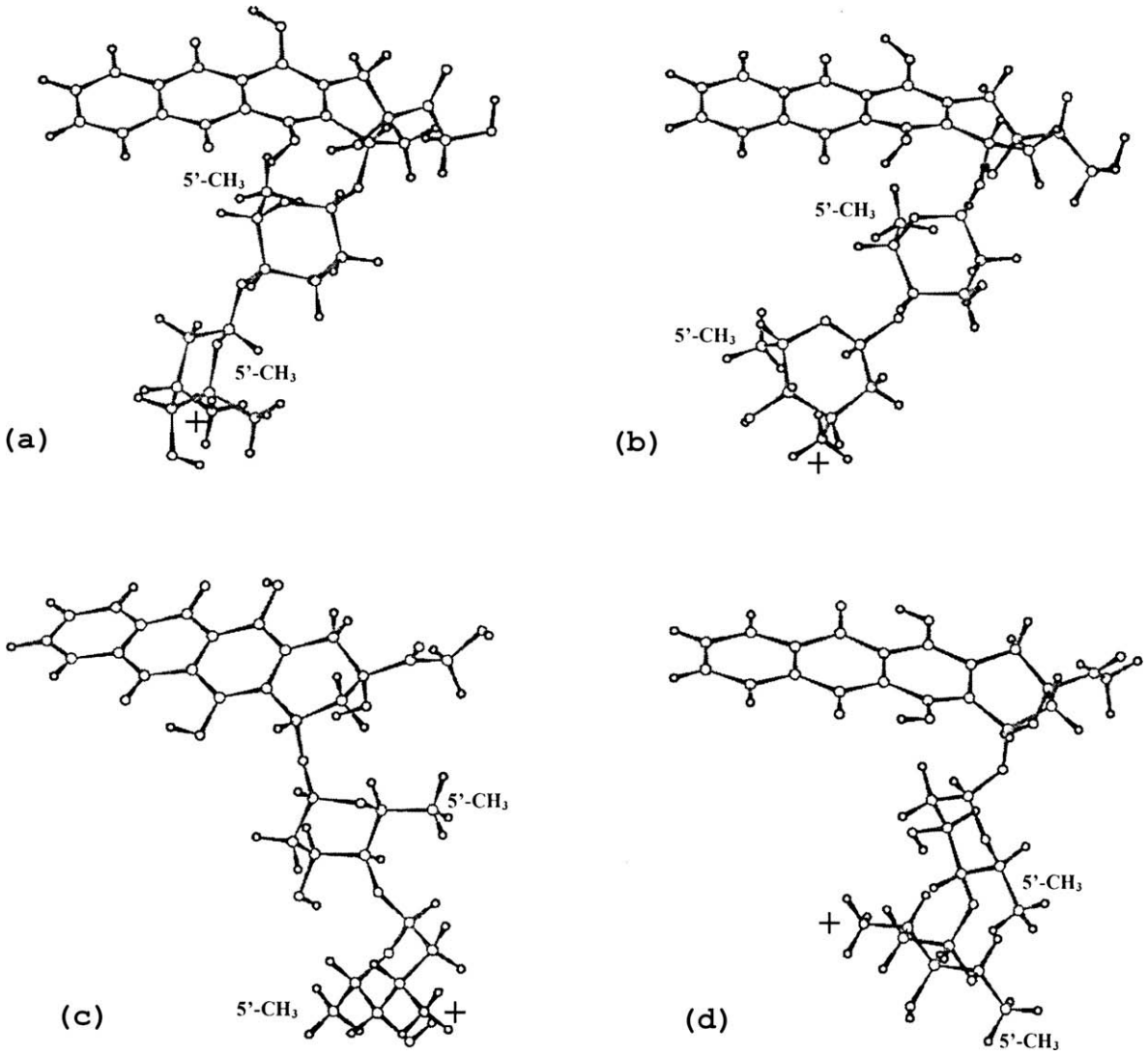

Figure 7. Comparison of the conformation of sabarubicin bound to AT in the (a) site 1 and (b) site 2; (c) preferred conformation of sabarubicin in the mono-intercalated complex with TA; (d) preferred conformation of Men10749 in the mono-intercalated complex with AT.

higher cytoplasmic/nuclear ratio and lower cellular uptake of sabarubicin in comparison with doxorubicin[31]and accordingly of the lower cytotoxicity of these disaccharide analogues. What are the reasons of such a short residence time? One reason certainly resides in the molecular structure of the DNA complexes. The enhanced flexibility of the daunosamine moiety in the disaccharides makes this unit less anchored to the minor groove of the helix. This is proved by the smaller conformational changes at the phosphate angles with respect to doxo, which are shown by the ^{31}P chemical shifts of the bound species and by the value of α and ζ phosphate angles derived by MD, especially for the mono-intercalated complexes.

The mono-intercalated complexes should be more favored than the bi-intercalated ones, compared with other anthracyclines, especially in the case of TA-complexes. This cannot be explained with an increased steric hindrance, owing to the presence of two sugar moieties, because nemorubicin, with a sugar ring plus a morpholino ring forms very stable bi-intercalated complexes. In this case, the morpholino ring strongly reduces the flexibility around the glycosidic bond, with the result of constraining the amino group anchored inside into the minor groove. The bi-intercalated complex of sabarubicin with AT was obtained with an excess of drug and with a solution of low ionic strength. The structure of this complex, determined on the basis of a relevant number of NOE interactions, shows the hydrophobic portion of both sugar rings, that is, the 5′-Me groups, located deeply into the minor groove, while the charged NH_3^+ group are on the boundary of the minor groove and can interact with the negative ionic surface of the helix and with the water molecules of the solvent. This differs from the X-ray structure, where the whole daunosamine ring at the second site protrudes out of the groove.

Actually, the bi-intercalated complexes have less biological relevance than the mono-intercalated ones, because in a polymeric DNA the presence of two intercalated drugs so close to each other is statistically improbable. Thus, a bi-intercalated complex with two drug molecules intercalated between the two top and the two bottom base pairs of a short oligonucleotide may not be a good model, as early noted by Pulmann.[32] Consequently, it is more informative to consider the dynamic process and observe what really occurs in solution, even in absence of the enzyme. The self-aggregation phenomenon, already known for anthracycline monosaccharides, is enhanced in the presence of oligonucleotides. The results of DOSY experiments showed for sabarubicin the most significant aggregation, which involves two duplex units in the case of TA complex. Doxorubicin binds one duplex, but some molecules are involved in outside binding to the helix; while nemorubicin

Table 6
Intermolecular NOE interactions and inter-proton distances (Å) for the complex of Men10755 with d(CGTACG)$_2$[a]

Men10755	d(CGTACG)$_2$		NOE[b]	d[c]
1,4-H	5-H	C_1	s	3.2[d]
1,4-H	6-H	C_1	s	3.6[d]
1,4-H	2′-H	C_1	w	4.4[d,g]
2,3-H	5-H	C_1	s	3.3[e]
2,3-H	6-H	C_1	w	5.2[e]
2,3-H	6-H	C_5	m	4.1[f]
2,3-H	2′-H	C_5	w	5.0[g]
8-CH_2	1′-H	G_6	w	5.0, 4.8
11-OH	5-H	C_1	m	4.9
11-OH	1′-H	C_1	w	5.2
11-OH	2′-H	C_1	s	2.5, 3.4
11-OH	1′-H	G_2	s	3.5
6-OH	1′-H	C_5	w[h]	4.3
6-OH	2′2″-H	C_5	s	3.0, 3.8
6-OH	8-H	G_6	m	4.5
6-OH	3′-H	G_6	m	4.9
2″-H(I)	5′-H	G_6	m	4.5, 3.1
5′-Me (I)	1′-H	T_3	m	4.5
5′-Me (I)	2′-H	T_3	w	4.4, 5.4
5′-Me (II)	1′-H	A_4	w	4.3
5′-Me (II)	5′-H	C_5	m	4.8, 4.9
5′-H (II)	1′-H	A_4	w	5.3
2′-H (II)	5′-H	A_4	w	4.7, 5.0
Relevant conformational energy parameters				
	E (kcal/mol)			
Forcing	1.7			
Van der Waals	−173.1			
Hydrogen-bond	−12.0			
Coulomb	−61.2			
Total	−63.0			
Distance violations (>0.3 Å)	1			

[a] Acquired at 10° C, 15 °C and 25 °C. Solvent D_2O and H_2O- D_2O (90:10 v/v), pH 6.7. The solution in D_2O was added of 10 mM phosphate buffer and 0.1 M NaCl.
[b] See footnote to Table 5.
[c] Obtained from the final structures of the complex after MD calculations.
[d] 1-H and 4-H are coincident, the distances are referred to 1-H.
[e] H-2 and H-3 are coincident, the distances are referred to 2-H.
[f] Distance referred to 3-H.
[g] The distance is referred to *pro-S*.
[h] With a contribution of secondary NOE.

showed no aggregation. The observed trend is interesting because is correlated with the structure of the complexes: the positive charge of nemorubicin is somehow shielded by the morpholino moiety and thus non available for external ionic interactions; in doxo, as well as in the disaccharide analogues, the positive charge of daunosamine ring is not constrained and can easily interact with the ionic surface of the duplex, forming outside binding, in addition to the intercalation.

Disaccharide analogues, lacking the amino group at C-3′ of fucose ring, are more flexible; in addition, the axial orientation of the daunosamine ring in sabarubicin makes the sugar moieties more extended, so much that the charged daunosamine ring of the bound drug, located at the external limit of the minor groove, can link each other the two duplexes. In the presence of topoisomerase II, the amino group could also bind the enzyme, thus favoring the stabilization of the so-called ternary cleavable complex, which is considered a required step for the activity, even though other factors may contribute to the improved antitumor efficacy observed for sabarubicin. Actually, the lengthening of the cationic arm with respect to the parent compound should enable it to reach the most satisfactory location for the interaction with the enzyme. The lower antitumor activity of Men10749, partially due to the presence of the daunomycin aglycone, might be correlated with a more difficult intercalation into the double helix. A second drug molecule cannot enter into the duplex (or the life time at the second site is extremely short) as suggested by the separation of solid material for $R = 1.5$. Actually, the equatorial binding of daunosamine at the fucose ring is responsible of the more closed shape of the disaccharide moiety, which is located inside into the minor groove. Consequently, the positively charged NH_3^+ group is close to the ribose oxygen atoms of the backbone, and thus not sufficiently exposed to link another duplex, as it occurs for sabarubicin.

4. Experimental

4.1. Sample preparation

The oligonucleotides, purified by HPLC, were purchased from Primm (Milan , Italy) and dissolved in D_2O (99.9% isotopic purity, Cambridge Isotope laboratories Inc.), or in H_2O/D_2O (90:10 v/v) at a 0.5–1 mM concentration range, in the presence or in the absence of 0.1 M NaCl, 10 mM and 20 mM phosphate buffer, pH 6.7. For NMR titration experiments stock solutions of the drugs were prepared at the concentration range of 10–14 mM.

4.2. NMR experiments

The NMR spectra were recorded on a Bruker AV600 spectrometer operating at a frequency of 600.10 MHz and 242.94 MHz, for ^1H, and ^{31}P nuclei, respectively. ^1H and ^{31}P spectra (broad-band ^1H decoupled mode) were recorded at variable temperature ranging from 5 °C to 45 °C. Chemical shifts (δ) were measured in ppm. ^1H and ^{31}P NMR spectra were referenced, respectively to external DSS (2,2-dimethyl-2-silapentane-5-sulfonate sodium salt) set at 0.00 ppm and MDA (methylenedisphosphonic acid) set at 16.8 ppm. Estimated accuracy for protons is within 0.02 ppm, for phosphorous is within 0.05 ppm.

^1H NMR titrations were performed at different temperatures, but the best results were obtained at 15 °C and 10 °C, by adding increasing amounts of the drug to the oligonucleotide solution until R = [drug]/[DNA] = 3.0 was reached. When the experiments are carried out in the presence of NaCl and phosphate buffer, both drugs began to precipitate from the solution, with $R = 2$ for sabarubicin, for $R = 1.5$ for Men10749. More successful were the experiments without salts: in H_2O the titration with sabarubicin could be carried out until $R = 3$ and the complex remained in solution, but Men10749 gave in general broader signals than sabarubicin. In the case of TA complexes, all the resonances became very broad and did not simplify at $R \geqslant 2$. The titration with sabarubicin in H_2O at 10 °C showed two signals for each OH proton of the drug and four signals for each imine NH protons of the bases and did not change with an excess of drug ($R = 3$). ^{31}P NMR titrations were performed in D_2O with salts at 25 °C, 15 °C and 5 °C. Sabarubicin with AT at 15 °C showed the appearance of a new signal at low field, which increased in intensity from $R = 0.5$ to $R = 2$. This signal was assigned to C_5 pG_6 by 2D NOESY-exchange. At $R = 1.5$ other new signals appeared at low field, which were assigned to G_2pA_3 and/or C_1pG_2. It was not possible to distinguish between each other, because their signals are overlapped in the free state and the spectrum of the complex is too broad. The titration on TA induces broadening with $R = 0.2$ at 25 °C as well as at lower temperatures. However, at 5 °C the resonance at low field of C_5pG_6 of the bound species could be detected. The titration with Men10749 was much more difficult: the very broad low field signal of C_5pG_6 was detected at 15 °C only in the case of AT complex.

^1H assignments for the drugs were performed by using NOESY and TOCSY experiments. The sequential assignments in free and bound oligonucleotides were performed by applying well established procedures for the analysis of double stranded B-DNA.[33] All the protons of the bound species were attributed for both sabarubicin and Men10749 (data reported in the Supplementary data). The ^1H and ^{31}P assignments for the free oligonucleotides d(CGTACG)$_2$

and $(CGATCG)_2$ have previously been reported.[21–23] Phase sensitive NOESY spectra were acquired at 25 °C, 15 °C and 10 °C in TPPI mode, with 4 K × 512 complex FIDs, spectral width of 8400 Hz and 15.000 Hz for D_2O and H_2O solutions, respectively, recycling delay of 1.5 s, 120 scans. Mixing times ranged from 50 ms to 300 ms. TOCSY spectra were acquired with the use of a MLEV-17[34] spin-lock pulse (field strength 10.000 Hz, 60 ms total duration). All spectra were transformed and weighted with a 90° shifted sine-bell squared function to 4 K × 1 K real data points. For samples dissolved in D_2O, water suppression was achieved by pre-saturation. For samples in H_2O, the 3-9-19 and the excitation sculpting sequences from standard Bruker pulse program libraries were employed. ^{31}P-2D-NOESY exchange experiments[19] were acquired (2 K × 320 FIDs, 420 scans) at different mixing times ranging from 50 to 300 ms.

Pseudo two-dimensional DOSY[28] experiments were acquired using the pulse-program 'stebpgp1s', diffusion delay: 0.12–0.45 s; gradient pulse: 1.5 ms; number of increments: 64. Raw data were processed using the standard DOSY software present in the Bruker library (TOPSPIN v. 1.3). A calibration curve was obtained using the following standards: glucose (MW 180; 3 mM in D_2O 99.9%; NaCl 0.1 M, phosphate buffer 10 mM, pH 6.7), $d(CGTACG)_2$ (MW 3754; 3 mM in D_2O 99.9%; NaCl 0.1 M, phosphate buffer 10 mM, pH 6.7), aprotinin (MW 6,500; 1 mM in D_2O 99.9%; pH 6.8), lysozyme (MW 14,400; 1 mM in D_2O 99.9%; pH 6.9), trypsin (MW 23,500; 1 mM in D_2O 99.9%; pH 3.0) and LCTI (*Lens culinaris* trypsin inhibitor) (MW 7447; 1 mM in D_2O 99.9%; pH 3.0).[35]

4.3. UV experiments

The UV spectra were recorded at 25 °C on a Perkin–Elmer Lambda 40 UV–vis spectrophotometer. UV titration experiments were performed following the variation of the λ_{max} of the sabarubicin (490 nm) by adding increasing amounts of the drug (1.47×10^{-3} M) to the oligonucleotide solution (7.0×10^{-4} M) until R = [drug]/[DNA] = 6.5 was reached.

4.4. Molecular modeling

Molecular models of $d(CGTACG)_2$, $d(CGATCG)_2$ and of drugs were built with Insight II & Discover (version 97.0 MSI, San Diego, CA) on a Silicon Graphics O2 workstation, using standard fragments from the Silicon Graphics library. The AMBER[36] as force-field was utilized without explicit inclusion of solvent molecules, setting a distance-dependent relative permittivity $\varepsilon = 4.0\,r$ and scaling the 1–4 non bond interactions by a factor of 0.5. For drugs, partial atomic charges were calculated using MOPAC[37] and the potentials were set by similarity with the DNA aromatic and sugar atoms. The models were energy minimized with a steepest-descendent followed by conjugate gradient algorithm. The drug-DNA complexes were then constructed following the NOE interactions. The observed NOEs were grouped into three intensity classes, corresponding to the following inter-proton distance intervals: s (strong) = 2.5–3.5 Å, m (medium) = 3.5–4.5 Å, w (weak) = 4.5–5.5 Å, estimated by using as reference the cross-peak of 5-H/6-H of cytidines (2.5 Å). Restraints were defined as quadratic well potentials with upper and lower limits on the basis of the above reported classes of NOE intensities with a force constant of 10 kcal · mol^{-1} $Å^{-2}$. The models were energy minimized and then a 100 ps of restrained MD simulation was performed at a constant temperature of 300 K. The average structure was subjected to a further minimization and taken as the starting structure for a subsequent 100 ps MD simulation at 300 K, sampling the trajectory every picosecond. The following restraints were applied: (i) hydrogen bonds between helical base pairs (except terminal base pairs); (ii) Drug–DNA interproton distances.

Acknowledgements

This work was supported by the University of Milano (Funds FIRST), and MURST (Funds PRIN-2005).

Supplementary data

Supplementary data associated with this article can be found, in the online version, at doi:10.1016/j.bmc.2010.01.012.

References and notes

1. Arcamone, F.; Doxorubicin Anticancer Antibiotics. In *Medicinal Chemistry series*; Academic Press: New York, 1981; Vol. 17, pp 1–369; Guidi, A.; Canarini, F.; Giolitti, A.; Pasqui, F.; Pestellini, V.; Arcamone, F. In *Anthracycline Antibiotics*; Priebe, W., Ed.; ACS Symposium Series; American Chemical Society: Washington, DC, 1995; Vol. 574, pp 47–58.
2. Zunino, F.; Capranico, G. *Anticancer Drug Des.* **1992**, *307*, 17.
3. Zunino, F.; Pratesi, G.; Perego, P. *Biochem. Pharmacol.* **2001**, *61*, 933.
4. Capranico, G.; Supino, R.; Binaschi, M.; Capolongo, L.; Grandi, M.; Sparato, A.; Zunino, F. *Mol. Pharm.* **1994**, *908*, 15.
5. Animati, F.; Arcamone, F.; Berrettoni, M.; Cipollone, A.; Franciotti, M.; Lombardi, P. *J. Chem. Soc., Perkin Trans.* **1996**, 1327.
6. Bargiotti, A.; Zini, P.; Penco, S.; Giuliani, F. US Patent 4672057, 1987.
7. Vasey, P. A.; Bisset, D.; Strolin-Benedetti, M.; Poggesi, I.; Breda, M.; Adams, L.; Wilson, P.; Pacciarini, M. A.; Kaye, S. B.; Cassedy, J. *Cancer Res.* **1995**, *55*, 2090.
8. Wassermann, K.; Markovits, J.; Jaxel, C.; Capranico, G.; Kohn, K. W.; Pommier, Y. *Mol. Pharm.* **1990**, *38*, 38.
9. Bortolini, R.; Mazzini, S.; Mondelli, R.; Ragg, E.; Ulbricht, C.; Penco, P. *Appl. Magn. Reson.* **1994**, *7*, 71.
10. Mazzini, S.; Mondelli, R.; Ragg, E. *J. Chem. Soc., Perkin Trans 2* **1998**, 1983.
11. Arcamone, F.; Animati, F.; Berrettoni, M.; Bigioni, M.; Capranico, G.; Casazza, A. M.; Camerini, C.; Cipollone, A.; De Cesare, M.; Franciotti, M.; Lombardi, P.; Madami, A.; Manzini, S.; Monteagudo, E.; Polizzi, D.; Pratesi, G.; Righetti, S. C.; Salvatore, C.; Supino, R.; Zunino, F. *J. Natl.Cancer Inst.* **1997**, *89*, 1217.
12. Pratesi, G.; De Cesare, M.; Camerini, C.; Perego, P.; Polizzi, D.; Supino, R.; Bigioni, M.; Manzini, S.; Iafrate, E.; Salvatore, C.; Casazza, A. M.; Arcamone, F.; Zunino, F. *Clin. Cancer Res.* **1998**, *4*, 2833.
13. Bigioni, M.; Benzo, A.; Irrisuto, C.; Lopez, G.; Curatella, B.; Maggi, C. A.; Manzini, S.; Crea, A.; Caroli, S.; Cubadda, F.; Binaschi, M. *Cancer Chemother. Pharmacol.* **2008**, *62*, 621.
14. Monteagudo, E.; Madami, A.; Animati, F.; Lombardi, P.; Arcamone, F. *Carbohydr. Res.* **1997**, *300*, 11.
15. Mondelli, R.; Ragg, E.; Fronza, G.; Arnone, A. *J. Chem. Soc., Perkin Trans. 2* **1987**, 15.
16. Ragg, E.; Ulbricht, C.; Mondelli, R.; Fronza, G.; Penco, S. *Gazz. Chim. Ital.* **1990**, *120*, 501.
17. Messori, L.; Temperini, C.; Piccioli, F.; Animati, F.; Di Bugno, C.; Orioli, P. *Bioorg. Med. Chem.* **2001**, *9*, 1815.
18. Temperini, C.; Messori, L.; Orioli, P.; Di Bugno, C.; Animati, F.; Ughetto, G. *Nucleic Acids Res.* **2003**, *31*, 1464.
19. Bodenhausen, G.; Ernst, R. R. *J. Am. Chem. Soc.* **1982**, *104*, 1304.
20. Gorenstein, D. J. *Chem. Rev.* **1994**, *94*, 1315.
21. Ragg, E.; Mondelli, R.; Battistini, C.; Garbesi, A.; Colonna, E. P. *FEBS Lett.* **1988**, 231.
22. Delepierre, M.; Huynh Dihn, T.; Proques, B. P. *Biopolymers* **1989**, *28*, 2115.
23. Lown, J. W.; Hanstock, C. C.; Bleackley, R. C.; Imbach, J. L.; Rayner, B.; Vasseur, J. J. *Nucleic Acids Res.* **1984**, *12*, 2519.
24. Chaires, J. B.; Dattagupta, N.; Crothers, D. M. *Biochemistry* **1982**, *21*, 3927.
25. Menozzi, M.; Valentini, L.; Tannini, E.; Arcamone, F. *J. Pharm. Sci.* **1984**, *73*, 766.
26. Chaires, J. B.; Dattagupta, N.; Crothers, D. M. *Biochemistry* **1985**, *24*, 260.
27. Rizzo, V.; Battistini, C.; Vigevani, A.; Sacchi, N.; Razzano, G.; Arcamone, F.; Garbesi, A.; Colonna, F. P.; Capobianco, M.; Tondelli, L. *J. Mol. Recognit.* **1989**, *2*, 132.
28. Morris, K. F.; Johnson, C. S., Jr. *J. Am. Chem. Soc.* **1992**, *114*, 3139.
29. Frederick, A.; Williams, L. D.; Ughetto, G.; van der Marel, J. H.; van Boom, J. H.; Rich, A.; Wang, A. H. J. *Biochemistry* **1990**, *29*, 2538.
30. Scaglioni, L.; Mazzini, S.; Mondelli, R.; Dallavalle, S.; Gattinoni, S.; Tinelli, S.; Beretta, G. L.; Zunino, F. *Bioorg. Med. Chem.* **2009**, *17*, 484.
31. Bigioni, M.; Salvatore, C.; Bullo, A.; Bellarosa, D.; Iafrate, E.; Animati, F.; Capranico, G.; Goso, C.; Maggi, C. A.; Pratesi, G.; Zunino, F.; Manzini, S. *Biochem. Pharmacol.* **2001**, *62*, 63.
32. Pullman, B. *Anti-Cancer Drug Des.* **1991**, *6*, 95.
33. Neuhaus, D.; Williamson, M. *The Nuclear Overhauser Effect in Structural and Conformational Analysis*; VCH: New York, 1998.
34. Bax, A.; Davis, D. G. *J. Magn. Reson.* **1985**, *65*, 355.
35. Ragg, E.; Galbusera, V.; Scarafoni, A.; Negri, A.; Tedeschi, G.; Consonni, A.; Sessa, F.; Duranti, M. *FEBS J.* **2006**, *273*, 4024.
36. Weiner, S. J.; Kollman, P. A.; Case, D. A.; Singh, U. C.; Ghio, C.; Alagona, G.; Profeta, S., Jr.; Weiner, P. *J. Am. Chem. Soc.* **1984**, *106*, 756.
37. Stewart, J. J. P. *J. Comput. Aided Mol. Des.* **1990**, *4*, 1.